AIAA JOURNAL
Vol. 34, No. 8, August 1996

Damage Localization in Structures Without Baseline Modal Parameters

Norris Stubbs*
Texas A&M University, College Station, Texas 77843
and
Jeong-Tae Kim†
National Fisheries University of Pusan, Pusan 608-737, Republic of Korea

A methodology to localize and estimate the severity of damage in structures for which only postdamage modal parameters are available for a few vibrational modes is presented. First, a theory of damage localization and severity estimation that utilizes only changes in mode shapes of the structures is outlined. Next, a system identification method that combines the experimental modal data and the modal parameters of a finite element model of the structure under investigation is developed to yield estimates of the baseline (i.e., predamage) modal parameters for the structure. Finally, the feasibility and practicality of the complete damage detection algorithm are demonstrated by localizing and sizing damage in a continuous beam for which only postdamage modal parameters for a single vibrational mode is available.

I. Introduction

As a result of collisions with foreign objects, fatigue loading, corrosive environments, etc., critical structural systems such as aircraft, spacecraft, bridges, and offshore platforms continuously accumulate damage in their service environments. For such structures, periodic inspections and maintenance are mandatory to ensure safety.[1] An accurate and reliable damage detection capability for such structures is essential since damage that is not detected and not repaired may lead to catastrophic structural failure.

During the past decade, a significant amount of research has been conducted in the area of damage detection using changes in modal parameters. Research studies have related changes in eigenfrequencies to changes in beam properties, such as cracks, notches or other geometrical changes.[2–4] Other studies have also focused on the possibility of using the vibration characteristics of structures as an indication of structural damage.[5–7] Since 1988, studies focusing on the vibrational approach to damage detection appear to be accelerating. Attempts have been made to monitor the structural integrity of bridges[8,9] and to investigate the feasibility of damage detection in aerospace structures using changes in modal parameters.[1,10–13]

Despite these research efforts, many problems related to damage detection remain unsolved. There are still outstanding needs to locate and estimate severity of damage 1) in structures for which only few modes are available, 2) in structures with many members, 3) in structures for which baseline modal responses are not available (i.e., the majority of existing structures), and 4) in an environment of uncertainty associated with modeling, measurement, and processing errors.

This paper presents a practical methodology to localize and estimate the severity of damage in structures for which only postdamage modal parameters are available for few vibrational modes (i.e., less than or equal to three modes and, in some cases, a single mode). To achieve the objective, we perform the following three tasks: 1) outline a theory (which utilizes changes in mode shapes of the structures) of damage localization and severity estimation, 2) summarize a system identification method that allows us to estimate a set of baseline modal parameters for a structure, and 3) demonstrate the feasibility and practicality of the complete procedure by localizing and sizing damage in a continuous beam for which only postdamage modal information on a single vibrational mode is available.

II. Damage Detection Algorithm

The minimum design requirements for the damage detection algorithm to be described include the following: 1) the algorithm should accurately localize the damage and 2) the algorithm should use minimum modal parameters.

A. Damage Localization Theory

Consider a linear, undamaged, skeletal structure with NE elements and N nodes. The ith modal stiffness K_i of the arbitrary structure is given by (see Refs. 10 and 14)

$$K_i = \boldsymbol{\Phi}_i^T \boldsymbol{C} \boldsymbol{\Phi}_i \tag{1}$$

where $\boldsymbol{\Phi}_i$ is the ith modal vector and $\boldsymbol{C}$ is the system stiffness matrix. The contribution of the jth member to the ith modal stiffness K_{ij} is given by

$$K_{ij} = \boldsymbol{\Phi}_i^T \boldsymbol{C}_j \boldsymbol{\Phi}_i \tag{2}$$

where $\boldsymbol{C}_j$ is the contribution of the jth member to the system stiffness matrix.

The fraction of modal energy for the ith mode that is concentrated in the jth member (i.e., the sensitivity of the jth member to the ith mode) is given by

$$F_{ij} = K_{ij}/K_i \tag{3}$$

Let the corresponding modal parameters in Eqs. (1–3) associated with a subsequently damaged structure be characterized by asterisks. Then for the damaged structure,

$$F_{ij}^* = \frac{K_{ij}^*}{K_i^*} = F_{ij}\left(1 + \sum_{k=1}^{NE} A_{ik}\alpha_k + \text{HOT}\right) \tag{4}$$

where K_{ij}^* and K_i^* are given by

$$K_{ij}^* = \boldsymbol{\Phi}_i^{*T} \boldsymbol{C}_j^* \boldsymbol{\Phi}_i^* \tag{5}$$

$$K_i^* = \boldsymbol{\Phi}_i^{*T} \boldsymbol{C}^* \boldsymbol{\Phi}_i^* \tag{6}$$

where A_{ik} is a set of coefficients associated with the mode i and location k, α_k the fraction of damage at location k in the structure,

Received June 24, 1994; revision received Oct. 19, 1995; accepted for publication Oct. 23, 1995.

*Professor, Mechanics and Materials Center, Department of Civil Engineering. Member AIAA.
†Assistant Professor, Department of Ocean Engineering.

and HOT the higher-order terms. On dividing Eq. (4) by Eq. (3), we obtain

$$F_{ij}^*/F_{ij} = \left(K_{ij}^*/K_{ij}\right)\left(K_i/K_i^*\right) \tag{7}$$

The quantities $\boldsymbol{C}_j$ and $\boldsymbol{C}_j^*$ in Eqs. (2) and (5) may be written as follows:

$$\boldsymbol{C}_j = E_j \boldsymbol{C}_{j0} \tag{8}$$

$$\boldsymbol{C}_j^* = E_j^* \boldsymbol{C}_{j0} \tag{9}$$

where the scalars E_j and E_j^* are parameters representing the material stiffness properties of undamaged and damaged jth member of the structure, respectively, and the matrix $\boldsymbol{C}_{j0}$ involves only geometric quantities (and possibly terms containing Poisson's ratio).

On comparing Eqs. (4) and (7), we make the following observations: 1) For each location we can write an equation for each mode. 2) If the damage is to be specified in a small region, then we will have a large number of equations to define the system. 3) We must find a way to determine the linear coefficients A_{ik} and the higher-order terms. Before we proceed as suggested earlier, we pose the following question: Is there a way to utilize Eq. (7) without having to determine A_{ik} and solve a large system of linear or nonlinear equations?

To provide an answer to the question, we resort to the following simplification. We have observed from experiment results (e.g., Ref. 15) that the geometry of mode shapes in the vicinity of an undamaged element of a structure changes very little when the structure is damaged elsewhere. It has also been experimentally observed that relative modal deformations (i.e., $\boldsymbol{\Phi}_i$) at a given location are larger after damage occurred (i.e., stiffness reduction occurs). Both of these observations are consistent (to a first approximation) with the approximation that the modal strain energy (F_{ij}) in an element remains the same before and after the damaging episode.

Consequently, we impose the approximation

$$F_{ij} = F_{ij}^* \tag{10}$$

Numerous numerical simulations have shown that this approximation holds for structures damaged simultaneously at multiple locations and at severity magnitudes of up to 30%. On substituting Eqs. (1), (2), (5), (6), (8), and (9) into Eq. (7) and rearranging, we obtain

$$\beta_j = \frac{E_j}{E_j^*} = \frac{\boldsymbol{\Phi}_i^{*T}\boldsymbol{C}_{j0}\boldsymbol{\Phi}_i^*}{\boldsymbol{\Phi}_i^T\boldsymbol{C}_{j0}\boldsymbol{\Phi}_i}\frac{K_i}{K_i^*} \tag{11}$$

in which the term β_j is the damage localization indicator for the jth member. If we set $K_i^* \approx \boldsymbol{\Phi}_i^{*T}\boldsymbol{C}\boldsymbol{\Phi}_i^*$, all quantities on the right-hand side (e.g., $\boldsymbol{\Phi}_i$ and $\boldsymbol{\Phi}_i^*$) can be obtained or approximated from modal parameters derived from experimental measurements and the geometry ($\boldsymbol{C}_{j0}$) of the structure. Note that if higher-order approximations [e.g., Eq. (4)] are made to relate F_{ij} and F_{ij}^*, more complicated expressions result from which it may be difficult to isolate inflicted damage from measurable model quantities.

From Eq. (11), damage is indicated at the jth member if $\beta_j > 1$. Note that if the jth member is at or near a node of ith mode, however, the denominator of Eq. (11) goes to zero (i.e., $F_{ij} \ll 1$), and a false prediction of damage results occurs. We overcome this limitation (i.e., that of a false positive prediction) in the following manner. Since $F_{ij} \ll 1$, adding unity to both sides of Eq. (10) yields

$$1 = \left(F_{ij}^* + 1\right)/\left(F_{ij} + 1\right) \tag{12}$$

Substituting for F_{ij}^* and F_{ij} using Eqs. (3) and (4) yields

$$1 = \frac{K_{ij}^* + K_i^*}{K_{ij} + K_i}\frac{K_i}{K_i^*} \tag{13}$$

Utilizing expressions for K_{ij}^* and K_{ij} in Eqs. (2) and (5) along with the relationships given in Eqs. (8) and (9), Eq. (13) is transformed to

$$1 = \frac{E_j^*}{E_j}\frac{\left(\boldsymbol{\Phi}_i^{*T}\boldsymbol{C}_{j0}\boldsymbol{\Phi}_i^* + \left(1/E_j^*\right)\sum_{k=1}^{NE}\boldsymbol{\Phi}_i^{*T}\boldsymbol{C}_k^*\boldsymbol{\Phi}_i^*\right)}{\left(\boldsymbol{\Phi}_i^T\boldsymbol{C}_{j0}\boldsymbol{\Phi}_i + (1/E_j)\sum_{k=1}^{NE}\boldsymbol{\Phi}_i^T\boldsymbol{C}_k\boldsymbol{\Phi}_i\right)}\frac{K_i}{K_i^*} \tag{14}$$

From which a new β_j may be defined as

$$\beta_j = \frac{\left(\boldsymbol{\Phi}_i^{*T}\boldsymbol{C}_{j0}\boldsymbol{\Phi}_i^* + \left(1/E_j^*\right)\sum_{k=1}^{NE}\boldsymbol{\Phi}_i^{*T}\boldsymbol{C}_k^*\boldsymbol{\Phi}_i^*\right)}{\left(\boldsymbol{\Phi}_i^T\boldsymbol{C}_{j0}\boldsymbol{\Phi}_i + (1/E_j)\sum_{k=1}^{NE}\boldsymbol{\Phi}_i^T\boldsymbol{C}_k\boldsymbol{\Phi}_i\right)}\frac{K_i}{K_i^*} \tag{15}$$

On substituting Eqs. (8) and (9) into Eq. (15), the damage localization indicator given a single mode is simplified as follows:

$$\beta_j = \frac{\left(\boldsymbol{\Phi}_i^{*T}\boldsymbol{C}_{j0}\boldsymbol{\Phi}_i^* + \left(1/E_j^*\right)\sum_{k=1}^{NE}\boldsymbol{\Phi}_i^{*T}E_k^*\boldsymbol{C}_{k0}\boldsymbol{\Phi}_i^*\right)}{\left(\boldsymbol{\Phi}_i^T\boldsymbol{C}_{j0}\boldsymbol{\Phi}_i + (1/E_j)\sum_{k=1}^{NE}\boldsymbol{\Phi}_i^T E_k\boldsymbol{C}_{k0}\boldsymbol{\Phi}_i\right)}\frac{K_i}{K_i^*}$$

$$\approx \frac{\left(\boldsymbol{\Phi}_i^{*T}\boldsymbol{C}_{j0}\boldsymbol{\Phi}_i^* + \sum_{k=1}^{NE}\boldsymbol{\Phi}_i^{*T}\boldsymbol{C}_{k0}^*\boldsymbol{\Phi}_i^*\right)}{\left(\boldsymbol{\Phi}_i^T\boldsymbol{C}_{j0}\boldsymbol{\Phi}_i + \sum_{k=1}^{NE}\boldsymbol{\Phi}_i^T\boldsymbol{C}_{k0}\boldsymbol{\Phi}_i\right)}\frac{K_i}{K_i^*} \tag{16}$$

If several modes (NM) are used to evaluate a potential damage location, we use the following formulation:

$$\beta_j = \frac{\sum_{i=1}^{NM}\left\{\left(\boldsymbol{\Phi}_i^{*T}\boldsymbol{C}_{j0}\boldsymbol{\Phi}_i^* + \sum_{k=1}^{NE}\boldsymbol{\Phi}_i^{*T}\boldsymbol{C}_{k0}\boldsymbol{\Phi}_i^*\right)K_i\right\}}{\sum_{i=1}^{NM}\left\{\left(\boldsymbol{\Phi}_i^T\boldsymbol{C}_{j0}\boldsymbol{\Phi}_i + \sum_{k=1}^{NE}\boldsymbol{\Phi}_i^T\boldsymbol{C}_{k0}\boldsymbol{\Phi}_i\right)K_i^*\right\}} \tag{17}$$

Next we establish more robust statistical criteria for damage localization. For a given set of modes, the locations of damage are selected on the basis of rejection of hypotheses in the statistical sense. First, the value β_j ($j = 1, 2, 3, \ldots, NE$) associated with each member is treated as a realization of a random variable β. In other words, the collection of the damage indices β_j represent a sample population. The normalized indicator is given by

$$Z_j = (\beta_j - \bar{\beta})/\sigma_\beta \tag{18}$$

in which the parameters $\bar{\beta}$ and σ_β represent the mean and the standard deviation of the indicators of β, respectively. The localization scheme used here essentially constitutes a detector that accepts a specific value of the damage index as input and provides as output a decision regarding the likelihood that the structure is damaged at that location. The null hypothesis is that the structure is not damaged at the jth member (i.e., H_0). If H_0 is true, we assume the distribution of the damage indices to be given by $f_\beta(\beta/H_0)$. The alternate hypothesis is that the structure is damaged at the jth member (i.e., H_1). For a given damage index β_j, the probability that the structure is not damaged at the jth member when H_1 is true is given by (see Ref. 16)

$$P_j = 1 - \int_0^{\beta_j} f_\beta \frac{\beta}{H_0}\,\mathrm{d}\beta \tag{19}$$

or the confidence that the jth member is a damaged location is $1 - P_j$.

B. Damage Severity Estimation Theory

Damage severity can be estimated directly from Eq. (11). Let the fractional change in the stiffness of the jth member be given by α_j, such that $\alpha_j \geq -1$, then by definition

$$E_j^* = E_j(1 + \alpha_j) \tag{20}$$

Combining Eqs. (11) and (20) yields

$$\alpha_j = \frac{\left[\boldsymbol{\Phi}_i^T\boldsymbol{C}_{j0}\boldsymbol{\Phi}_i\right]}{\left[\boldsymbol{\Phi}_i^{*T}\boldsymbol{C}_{j0}\boldsymbol{\Phi}_i^*\right]}\frac{K_i^*}{K_i} - 1 \tag{21}$$

Note that the use of Eq. (10) will result in an overestimate of the damage severity because here we estimate Eq. (6) by the equation $K_i^* \cong \boldsymbol{\Phi}_i^{*T}\boldsymbol{C}\boldsymbol{\Phi}_i^*$ but in reality $|\boldsymbol{C}| > |\boldsymbol{C}^*|$. Note also that we estimate K_i^* in this manner[1] since the damage location and severity are assumed to be unknown.

III. System Identification Method

By definition, a baseline structure is a structure with the same topology as the one given minus the damage accumulated over the period of interest. It is impossible to know with complete certainty the initial stiffness and mass distribution of the pristine structure. Given a knowledge of the structure and engineering judgement, however, we can propose possible pristine structures. In the cases of simple structures such as beams, we can make such judgements with great certainty. In the cases of more complicated structures, our confidence to propose a related pristine structure will depend on the availability of as-built documentation on the structure. Once a pristine structure has been proposed, techniques from system's identification along with the dynamic response of the postdamaged structure can be used to evaluate the defining parameters of the pristine structure.

Here we address the following problem: develop a system identification method to generate baseline modal parameters of a structure for which only a set of postdamage modal parameters are available. We provide a solution to the problem in two steps: 1) propose a generic finite element model of the baseline structure and 2) use the experimental data from the postdamage structure to calibrate the generic finite element model.

Consider a linear skeletal structure with NE members and N nodes. Suppose $\boldsymbol{k}_j^*$ is the unknown stiffness of the jth member of the structure for which M measured eigenvalues are known. Also, suppose $\boldsymbol{k}_j$ is a known stiffness of the jth member of a finite element (FE) model for which the corresponding set of M computed eigenvalues are known. Then, relative to the FE model, the fractional stiffness change of the jth member of the structure α_j and the stiffnesses ($\boldsymbol{k}_j$ and $\boldsymbol{k}_j^*$) are related according to the equation

$$\boldsymbol{k}_j^* = \boldsymbol{k}_j(1+\alpha_j) \tag{22}$$

The fractional stiffness change of NE members may be obtained using the following equation (see Ref. 10 for details):

$$\alpha = \boldsymbol{F}^{-1}\boldsymbol{Z} \tag{23}$$

where α is a $NE \times 1$ matrix containing the fractional changes in stiffnesses between the FE model and the structure, $\boldsymbol{Z}$ is a $M \times 1$ matrix containing the fractional changes in eigenvalues between the two systems, and $\boldsymbol{F}$ is a $M \times NE$ damage sensitivity matrix relating the fractional changes in stiffnesses to the fractional changes in eigenvalues.

The $M \times NE$ matrix $\boldsymbol{F}$ can be determined as follows. First, M undamaged eigenvalues are numerically generated for a reference FE model of the structure. Second, a known severity of damage (α_k) at member k of the FE model is introduced and M damaged eigenvalues are numerically generated. Third, the fractional changes between the M undamaged eigenvalues and M damaged (at member k) eigenvalues are computed. Fourth, each component of the kth column of the $\boldsymbol{F}$ matrix (i.e., the $M \times 1$, matrix $\boldsymbol{F}$) is computed by dividing the fractional changes in each eigenvalue by the simulated severity at the member k. Finally, the $M \times NE$ matrix $\boldsymbol{F}$ is generated from repeating the whole procedure for all NE damage locations.

With the $\boldsymbol{F}$ matrix generated, the following 7-step algorithm is proposed to identify a given structure:

1) Select the target structure (i.e., a postdamage state of the structure).

2) Derive an FE model of the structure.

3) Compute the damage sensitivity matrix for the FE model.

4) Compute the fractional changes in eigenvalues between the FE model and the target structure.

5) Fine tune the FE model by first solving Eq. (23) to estimate stiffness changes (i.e., to compute the $NE \times 1$ matrix α) and next solving Eq. (22) to update the stiffness parameters of the FE model.

6) Repeat steps 1–5 until $\boldsymbol{Z} \cong 0$ or $\alpha \cong 0$ (i.e., as they approach zero).

7) Estimate the mass matrix of the structure from the knowledge of the geometry or materials that comprise the structure.

The values of $\boldsymbol{k}_j^*$ $(j = 1, 2, \ldots, NE)$ and the mass matrix define the baseline structure. Once the FE model is identified, modal parameters of the FE model can be numerically generated by performing a dynamic analysis.

IV. Damage Detection in a Continuous Beam

In this section, the feasibility and practicality of the proposed damage detection scheme is demonstrated by localizing and sizing damage in a continuous beam for which only postdamage modal parameters are available for a single mode of vibration. This objective is accomplished in five steps: 1) the test structure is described; 2) the extraction of modal parameters for the test structure is described; 3) baseline modal parameters of the test structure are identified using the system identification method; 4) a damage detection model (i.e., a mathematical representation of a structure with degrees of freedom corresponding to sensor readings) of the test structure is selected; and 5) damage localization and severity estimation in the test structure is performed, using the proposed damage detection theory.

A. Description of the Test Structure

Mazurek and DeWolf[15] conducted controlled laboratory experiments on a two-span continuous beam on elastic supports to investigate the relationship between changes in modal response parameters and structural degradation of the beam. The test structure (the two-span aluminum beam schematized in Fig. 1) consisted of plates and angle shapes bolted together to form two I-section beams. The beams were joined together by cross ties on the top and the bottom chords, as shown in Fig. 1, forcing the structure to act essentially as a box-shape beam. The structure had three supports: a pin support 6 in. (0.15 m) from the left edge, a roller support at the middle, and another roller support 6 in. (0.15 m) from the right edge. Placement of the 11 accelerometers was along the centerline of the beam. Ambient forces from lightweight traffic carts excited the structure. Frequency response functions were generated from the acceleration-time histories and modal characteristics were determined using the polynomial curve-fit approach (see Ref. 17).

B. Description of Measured Modal Parameters of the Test Structure

The extracted modal parameters of the test structure included predamage and postdamage mode shapes of the first bending mode and resonant frequencies of the first three bending modes (in this paper we ignore the measured predamage modal parameters). A known damage (shown in Fig. 1) was inflicted in the structure by cracking the beam at a location 40 in. (1.02 m) to the left of the right support. The crack (i.e., the inflicted damage) was placed on the right web shown in Fig. 1. The crack was developed further by sequentially reducing the second moment of area at the damaged location to about 81% (stage 1), 68% (stage 2), and 67% (stage 3) of the original cross section (note that these damage stages correspond to reducing the bending stiffness at the damaged section to 19, 32, and 33%). The measured resonant frequencies are listed in Table 1 and the extracted mode shapes of the first mode are shown in Fig. 2.

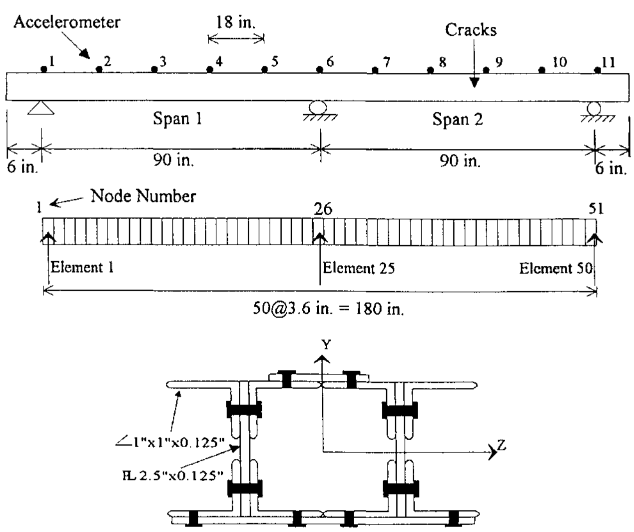

Fig. 1 Schematic of the test structure.

Table 1 Resonant frequencies of the test structure

Damage case	Resonant frequency, Hz Mode 1	Mode 2	Mode 3
Predamage	32.32	46.58	118.1
Stage 1	32.02	45.98	116.1
Stage 2	30.96	45.38	115.7
Stage 3	29.01	45.07	115.5

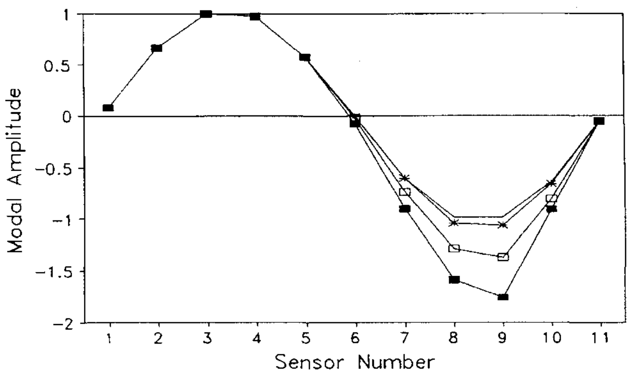

Fig. 2 First bending mode shapes for the test structure.

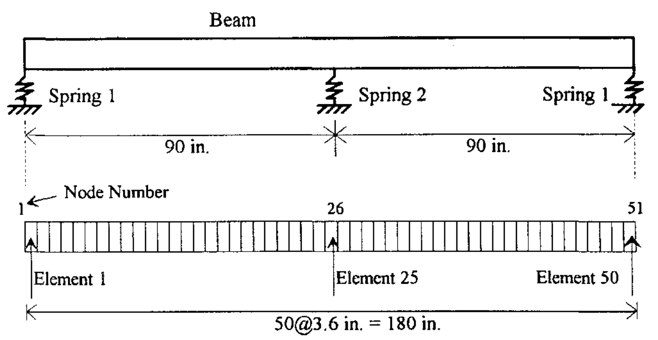

Fig. 3 Schematic of the FE model of the test structure.

Note that these mode shapes were obtained by digitizing the original mode shapes presented in Ref. 15.

C. Identification of Baseline Modal Parameters

The baseline modal parameters (i.e., frequencies and mode shapes of the undamaged state) of the test structure were identified by using the system identification algorithm described earlier. In step 1 we selected the first damage state of the structure (i.e., stage 1) as the target structure. The first damage stage was selected because in the real world, only a single postdamage case might be available. The frequencies of the first three modes of the target structure are listed in Table 1. In step 2, we selected an FE model of the test structure as an initial guess. As shown in Fig. 3, the FE model consisted of three member types: member type 1 [the 50 equally sized, three-dimensional frame elements (of uniform stiffness and mass) that model the beam]; member type 2 [the two outside axial springs (spring 1)]; and member type 3 [the middle axial spring (spring 2)]. Note that supports for the FE model are modeled as axial springs. Our reasons for not modeling supports as rigid are as follows. On examining the experimentally determined mode shapes in Fig. 2, note that displacements at the end and middle supports are not zero. Thus supports in the real structure are not rigid in comparison to the flexural rigidity of the beam.

Consequently, to identify the baseline model we need to specify three stiffness parameters: the stiffness of the beam elements, the stiffness of the outer springs, and the stiffness of the middle support. Initial values for the geometric properties of the FE model were estimated as follows. For member type 1, $A = 1.625$ in.^{2} (0.05×10^{-3} m^2), the second moment of area with respect to z axis (shown in Fig. 1) $I_z = 1.737$ in.^{4} (7.23×10^{-7} m^4), and the second moment of area with respect to y axis (shown in Fig. 1) $I_y = 3.990$ in.^{4} (9.59×10^{-2} m^4). For member types 2 and 3, $A = 0.1$ in.^{2} (6.45×10^{-5} m^2) and $I_y = I_z \approx 0$. Material properties of the FE model were assigned as 1) the elastic modulus $E = 10 \times 10^6$ psi (70 GPa), 2) Poisson's ratio $\nu = 0.33$, and 3) the linear mass density $\rho = 2.537 \times 10^{-4}$ lb $\cdot$ s^2/in.^{4}(2710 kg/m^3). The stiffness parameters of the FE model selected to be fine-tuned were the stiffness matrix of a three-dimensional frame element for member type 1 and the axial rigidity (EA) for member types 2 and 3. In step 3 we computed a 3×3 (i.e., 3 modes and 3 member types) sensitivity matrix of the FE model. As listed in Table 2, for a given mode, an element sensitivity represents the fraction of modal strain energy of that particular element group. In step 4 we computed the fractional changes in eigenvalues between the FE model (i.e., the initial guess) and the target structure (i.e., the first damage case in the test structure). The eigenvalues of the first three modes for the FE model were computed using the software package ABAQUS.[18] In step 5 we fine-tuned the FE model. This step was accomplished by first solving Eq. (23) to estimate the stiffness parameters of the three members, then solving Eq. (22) to update the stiffness parameters of the same members.

Table 2 Sensitivity matrix to fine tune the FE model

Mode	Sensitivity of member types Type1	Type 2	Type 3
1	0.9995	0.5E-3	0.1E-4
2	0.9950	0.1E-2	0.4E-2
3	0.9979	0.2E-2	0.1E-3

Table 3 Values of frequencies (hertz) for 10 iterations

Mode number	Initial guess	Iteration number 2	4	6	8	10	Target values
1	39.76	32.63	32.54	32.45	31.37	32.29	32.02
2	61.99	44.60	45.15	45.47	45.63	45.76	45.98
3	158.75	121.32	120.07	119.18	118.15	117.13	116.10

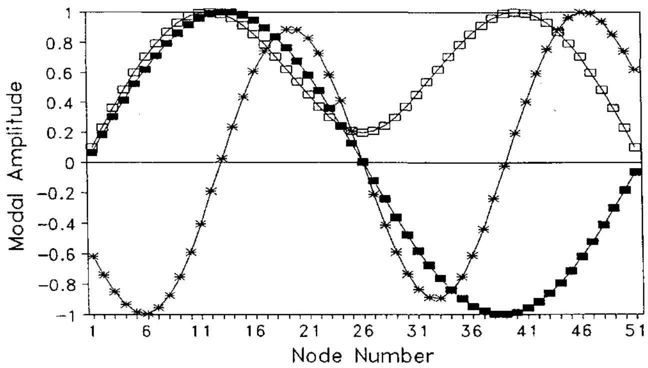

Fig. 4 Identified mode shapes of the baseline structure.

The results, using frequencies of the first three modes and 10 iterations, are listed in Table 3. Note that after 10 iterations the identified frequencies were within 1% of the target values. We therefore selected the structure defined by the 10th iteration as the baseline structure. Thus the modal parameters associated with the latter structure became the modal parameters of the baseline structure. The mode shapes of the first three modes for the identified baseline structure are shown in Fig. 4.

Next, we examined the correlation between the first bending mode shape ($u \in R^N$) of the target structure as shown in Fig. 2 and the identified mode shape ($v \in R^N$) of the baseline structure as shown in Fig. 4. Note that R^N is the space of order N. Given the two sets of the mode shape, we computed the modal assurance criterion (MAC), which is defined as (see Ref. 17 for details)

$$\mathrm{MAC}\,(\boldsymbol{u}, \boldsymbol{v}) = \frac{(\boldsymbol{u}, \boldsymbol{v})^2}{(\boldsymbol{u}, \boldsymbol{u})(\boldsymbol{v}, \boldsymbol{v})} \tag{24}$$

The MAC for the two mode shapes equals 0.9989 indicating the high degree of correlation between the modes. Note that even though the two mode shapes are highly correlated, the two underlying structures are different. The target structure is damaged at a specific location whereas the baseline structure has uniform stiffness throughout its length.

D. Damage Detection Model of the Test Structure

As a damage detection model (DDM) of the test structure, we selected an Euler–Bernoulli beam model because the test structure is a box-shape beam and the extracted modal data provide information to model a one-dimensional structure. As shown in Fig. 1, the damage detection model consisted of 50 beam elements of equal size. The fraction of modal energy for the Euler–Bernoulli beam model [i.e., the equivalent expression for the right-hand side of Eq. (3)] of element k and mode i between two locations $(x_k, x_k + \Delta x_k)$ was computed using

$$F_{ik} = \int_{x_k}^{x_k+\Delta x_k} EI_z\{\phi_i''(x)\}^2 \frac{\mathrm{d}x}{K_i} \qquad \left[K_i = \int_0^L EI_z\{\phi_i''(x)\}^2\,\mathrm{d}x\right] \tag{25}$$

The elastic modulus and the second moment of area about the z axis (shown in Fig. 1) for the 50 uniform elements were estimated as $E = 10 \times 10^6$ psi (70 Gpa) and $I_z = 1.737$ in.^{4} (7.23×10^{-7}m^4) respectively. Next, the curvatures of the mode shapes were generated at the 51 nodes of the DDM (note that each mode shape shown in Fig. 2 contained only 11 sensor readings). The curvatures were obtained as follows: 1) modal amplitudes corresponding to nodes 1–51 were estimated by interpolating, using cubic-spline functions, the 11 data points of the mode shapes shown in Fig. 2; 2) a modal displacement function $w(x)$ was generated for the entire structure using third-order interpolation functions; and 3) the curvatures [i.e., $\phi''(x)$] were determined at the 51 nodes.

E. Damage Localization and Severity Estimation in the Test Structure

We located and estimated the severity of damage in the test structure for the three damage stages described. First, as the input to the damage detection model [i.e., the Euler–Bernoulli beam model for which the fraction of modal strain energy is given by Eq. (25)], we selected the first bending mode shape. Note that the postdamage mode shapes are shown in Fig. 2 and the baseline mode shape is shown in Fig. 4. Second, we computed the damage localization indicator [given by Eq. (17)] of the damage detection model. Third, we established the damage localization criterion for Eq. (18) as follows: select H_0 (i.e., no damage exists at member i) if $Z_i < 2$ and select the alternate H_1 if $Z_i \geq 2$. Note that this criterion corresponds to a one-tailed test at a significance level of 0.023 (97.7% confidence level). Fourth, we used the latter criterion to select potential damage locations. The inflicted and predicted damage locations for the three damage stages are shown in Fig. 5. Finally, damage severity at each predicted damage location was estimated by using the severity estimator [given by Eq. (21)]. The estimated severities of damage are listed in Table 4.

From the damage localization results (shown in Fig. 5) and the severity estimation results (listed in Table 4) of the test structure, the following four observations can be made. First, for all levels of damage (i.e., stage 1 to stage 3), damage (at element 39) is correctly localized. Second, the locations of false-positive predictions are always adjacent (or near) to element 39. Third, the precision (the decreasing size of the predicted damaged region) of the damage localization scheme increases as the level of the inflicted damage increases. For example, from Fig. 5, in damage stages 1–3, the predicted locations were, 39–42, 39–42, and 39–41, respectively. Finally, the predicted severity estimation results consistently overestimate the inflicted damage. The following conclusions are based on these results: 1) the proposed methodology can accurately localize damage in a real structure and 2) the methodology for the estimation of the damage severity approximates but tends to overestimate the magnitude of damage.

Table 4 Severity estimation results of the test structure

Damage case	Damage locations	Magnitude(s) of damage	
		Inflicted, %	Predicted, %
Stage 1	39	−19	−21
Stage 2	39	−32	−55
Stage 3	39	−33	−69

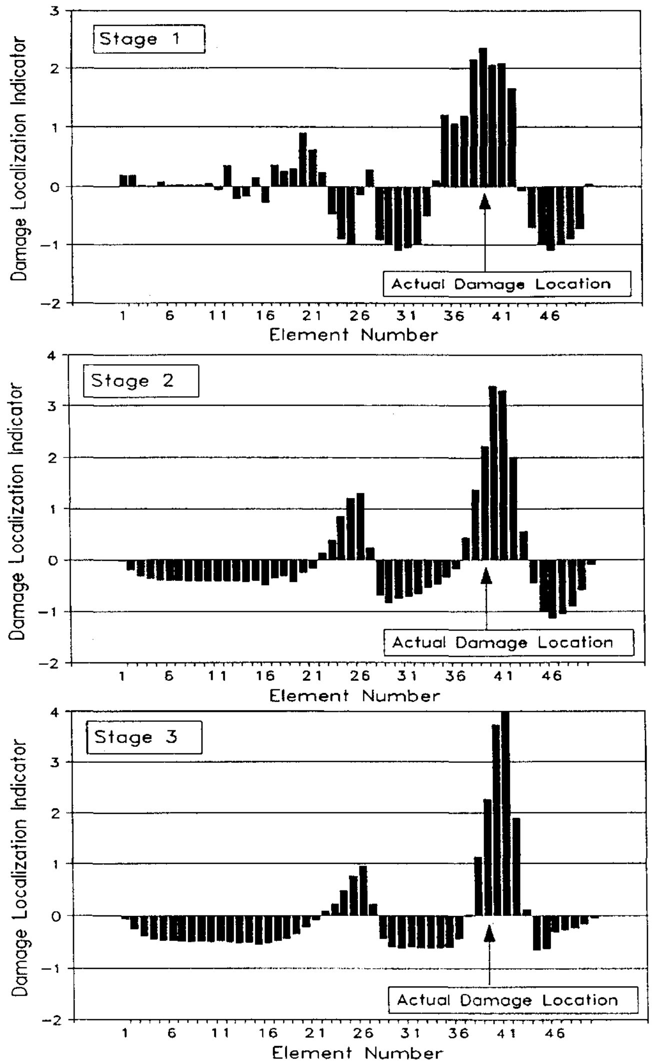

Fig. 5 Damage localization results of the test structure.

V. Summary and Conclusions

This paper presents a practical methodology to localize and estimate the severity of damage in structures for which only postdamage modal parameters were available for one to three modes of vibration. The proposed methodology is presented in three parts. The first part outlined a theory of damage localization and severity estimation that yielded information on the location and severity of damage directly from changes in mode shapes of the structures. The second part formulated a system identification method that identified baseline modal parameters of the structures. The third part demonstrated the feasibility and practicality of the damage detection algorithm by accurately localizing and approximately sizing damage in a continuous beam for which only postdamage modal parameters for a single vibrational mode were available.

We conclude that it is possible to localize damage and estimate the severity of damage in a structure with knowledge of only postdamage mode shapes of very few vibrational modes (in this study, only one mode) and a finite element model identifying the undamaged state of the structure. Research to improve the damage detection algorithm presented is continuing along three lines of inquires. First, we are developing algorithms to more accurately estimate the size of damage. Second, we are extending the algorithm to more complicated structures such as three dimensional frames. Third, we are now in advanced stages of demonstrating the practicality of the approach in damage localization and severity estimation in full-scale field structures.[19]

References

[1]Chen, J., and Garba, J. A., "On-Orbit Damage Assessment for Large Space Structures," *AIAA Journal*, Vol. 26, No. 9, 1988, pp. 1119–1126.

[2]Gudmunson, P., "Eigenfrequency Changes of Structures Due to Cracks, Notches or Other Geometrical Changes," *Journal of Mechanics and Physics of Solids*, Vol. 30, No. 5, 1982, pp. 339–353.

[3]Gudmunson, P., "The Dynamic Behavior of Slender Structures with Cross-Sectional Cracks," *Journal of Mechanics and Physics of Solids*, Vol. 31, No. 4, 1983, pp. 329–345.

[4]Cristides, S., and Barrs, A. D. S., "One-Dimensional Theory of Cracked Bernoulli-Euler Beams," *International Journal of Mechanical Science*, Vol. 26, No. 11/12, 1984, pp. 639–648.

[5]Adams, R. D., Cawley, P., Pye, C. J., and Stone, B. J., "A Vibration Techniques for Non-Destructively Assessing the Integrity of Structures," *Journal of Mechanical Engineering Science*, Vol. 20, No. 2, 1978, pp. 93–100.

[6]Cawley, P., and Adams, R. D., "The Location of Defects in Structures from Measurements of Natural Frequencies," *Journal of Strain Analysis*, Vol. 14, No. 2, 1979, pp. 49–57.

[7]O'Brien, T. K., "Stiffness Change as a Nondestructive Damage Measurement," *Mechanics of Non-Destructive Testing*, edited by W. W. Stinchcomb, Plenum, New York, 1980, pp. 101–121.

[8]Biswas, M., Pandey, A. K., and Samman, M. M., "Modal Technology for Damage Detection of Bridges," *NATO Advanced Research Workshop on Bridge Evaluation, Repair and Rehabilitation*, edited by A. Nowak, Kluwer Academic, Boston, MA, 1990, pp. 161–174.

[9]Flesch, R. G., and Kernichler, K., "Bridge Inspection by Dynamic Tests and Calculations Dynamic Investigations of Lavent Bridge," *Workshop on Structural Safety Evaluation Based on System Identification Approaches*, edited by H.G. Natke and J. T. P. Yao, Vieweg, Lambrecht/Pfalz, Germany, 1988, pp. 433–459.

[10]Stubbs, N., and Osegueda, R., "Global Non-Destructive Damage Evaluation in Solids," *International Journal of Analytical and Experimental Modal Analysis*, Vol. 5, No. 2, 1990, pp. 67–79.

[11]Hajera, P., and Soeiro, F. J., "Structural Damage Detection Based on Static and Modal Analysis," *AIAA Journal*, Vol. 28, No. 2, 1990, pp. 1110–1115.

[12]Kaouk, M., and Zimmerman, D., "Structural Damage Assessment Using a Generalized Minimum Rank Perturbation Theory," *AIAA Journal*, Vol. 32, No. 4, 1994, pp. 836–842.

[13]Sheinman, I., "Damage Detection in Framed Structures," *AIAA Journal*, Vol. 32, No. 5, 1994, pp. 1103–1105.

[14]Stubbs, N., Kim, J. T., and Topole, K., "An Efficient and Robust Algorithm for Damage Localization in Offshore Platforms," *ASCE Tenth Structures Congress '92* (San Antonio, TX), American Society of Civil Engineers, New York, 1992, pp. 543–546.

[15]Mazurek, D. F., and DeWolf, J. T., "Experimental Study of Bridge Monitoring Technique," *Journal of Structural Engineering*, Vol. 116, No. 9, 1990, pp. 2532–2549.

[16]Gibson, J. D., and Melsa, J. L., *Introduction to Nonparametric Detection with Applications*, Academic, New York, 1975.

[17]Ewins, D. J., *Modal Testing: Theory and Practice*, Research Studies Press, Letchworth, England, UK, 1986.

[18]Anon., "ABAQUS User Manual," Hibbitt, Karlsson and Sorensen, Inc., 1992.

[19]Stubbs, N., Kim, J. T., and Farrar, C. R., "Field Verification of a Nondestructive Damage Localization and Severity Estimation Algorithm," *Proceedings of the 13th International Modal Analysis Conference* (Nashville, TN), Society for Experimental Mechanics, Bethel, CT, 1995, pp. 210–218.